Effect of Hydrothermal Conditions on Structural and Textural Properties of Synthetic Hydrotalcites of Varying Mg/Al Ratio

Sumeet K. Sharma, Pushpendra K. Kushwaha, Vivek K. Srivastava, Sharad D. Bhatt, and Raksh V. Jasra*

Discipline of Inorganic Materials and Catalysis, Central Salt and Marine Chemicals Research Institute (CSMCRI), G.B. Marg, Bhavnagar−364 002, Gujarat, India

The synthetic hydrotalcites with Mg/Al molar ratios of 2.0−3.5 were synthesized by coprecipitation method at low supersaturation conditions followed by hydrothermal treatment under autogenous water vapor pressure at 70−140 °C. These synthesized samples were characterized by powder X-ray diffraction (P-XRD), Fourier transform infrared spectroscopy (FT-IR), thermogravimetric analysis (TGA), scanning electron microscopy (SEM), and surface area measurements. The hydrothermal treatment at increasing temperature and longer aging time increased the crystallinity and crystallite size of the hydrotalcite significantly. The crystallinity and crystallite size of the hydrotalcite were observed to decrease on increasing the Mg/Al ratio. The surface area of hydrotalcite was observed to increase on increasing the Mg/Al molar ratio from 2.0 to 3.5. From the kinetic data for crystallization of hydrotalcite at different temperatures, the values of rate constants and activation energy were calculated. The Avrami−Erofeev model (nucleation-growth model) was used for fitting the crystallization data.

Introduction

Hydrotalcites[1] have received much attention in view of their potential applications as adsorbents, as anion exchangers, in nucleophilic halide exchange, and, more importantly, in heterogeneous catalysis as catalysts and catalyst support for a variety of organic transformations such as aldol condensation, Claisen−Schmidt condensation, Knovengel condensation, isomerization, alkylation of diketones, and epoxidation of activated olefins with hydrogen peroxide.[2−15] The most commonly used method for the synthesis of hydrotalcite involves coprecipitation of metal salt solutions at low supersaturation and constant pH ranging from 7 to 10 in the temperature range of 60−80 °C.[1] The important parameters determining the applications of hydrotalcites are degree of crystallinity and textural properties. These properties are influenced by various parameters such as the nature of the bivalent and trivalent cations and their ratio, the nature of the anions, the concentrations of metal salt solution and alkali solution, the rate of addition of metals and alkali solutions, the reaction pH, the aging temperature and time, and the drying temperature of the obtained precipitate. The specific surface area, morphology, and particle-size distribution of the hydrotalcite also depend on the synthesis method.[16] Numerous studies on the physicochemical properties, the applications of hydrotalcite, and the thermal stability of various hydrotalcites are reported,[17−22] but limited literature is available on the control of structural and textural properties of hydrotalcite, which play an important role for catalytic as well as material applications.[23−26] For example, Miyata reported[23] the effect of hydrothermal treatment temperature on crystallite size of the hydrotalcite. The crystal size of the hydrotalcite was reported to increase up to 180 °C hydrothermal treatment temperature followed by a decrease above 200 °C. Hickey et al. confirmed the formation of the hexagonal plate-shaped crystals of the hydrotalcite under hydrothermal treatment conditions using transmission electron microscopy (TEM) at different aging temperatures.[24] The effect of the aging time on crystallinity of hydrotalcite at constant hydrothermal treatment temperature was studied by Rives and co-workers.[25] The effect of hydrothermal treatment on the crystallinity of synthetic hydrotalcite at a Mg/Al molar ratio of 2 was studied by Kovanda et al. in the 120−200 °C temperature range.[26] The literature is largely confined to the study of the effect of hydrothermal treatment on structural properties like crystallinity, crystallite size, and particle size of hydrotalcite at a Mg/Al molar ratio of 2.0 or 3.0. The literature is sparse on the study of the effect of varying Mg/Al molar ratios of hydrotalcite on the crystallization, kinetics of crystallization, and textural properties under varying hydrothermal treatment conditions.

The aim of the present investigation is to study the effect of hydrothermal treatment temperature and crystallization kinetics on structural and textural properties of synthetic hydrotalcites of varying Mg/Al molar ratios (2.0, 2.5, 3.0, and 3.5).

Experimental Section

Materials. Magnesium nitrate, $Mg(NO_3)_2 \cdot 6H_2O$, 99.99%, and aluminum nitrate, $Al(NO_3)_3 \cdot 9H_2O$, 99.99%, sodium carbonate (Na_2CO_3, 99.99%), and sodium hydroxide (NaOH, 99.99%) were purchased from s.d. Fine Chemicals, India, for the synthesis of hydrotalcite. The double-distilled millipore deionized water was used during the synthesis.

Synthesis of Hydrotalcites by Coprecipitation Method. The magnesium−aluminum hydrotalcite samples having a Mg/Al molar ratio from 2.0 to 3.5 were synthesized by coprecipitation method at constant pH under low supersaturation conditions. Typically, for the synthesis of hydrotalcite sample with a Mg/Al molar ratio = 2.5, an aqueous solution of $Mg(NO_3)_2 \cdot 6H_2O$ (0.22 mol) and $Al(NO_3)_3 \cdot 9H_2O$ (0.088 mol) in 200 mL double-distilled deionized water and aqueous solution (200 mL) containing NaOH (0.72 mol) and Na_2CO_3 (0.21 mol) were added slowly (in around 2 h) to a 1 L round-bottom flask under vigorous stirring at room temperature. The contents of the flask were then transferred into the Teflon coated stainless steel autoclave for hydrothermal treatment at predefined temperature

* To whom correspondance should be addressed. E-mail: rvjasra@csmcri.org. Tel.: +91 278 2471793. Fax: +91 278 2567562.

10.1021/ie061438w CCC: $37.00
Published on Web 06/14/2007

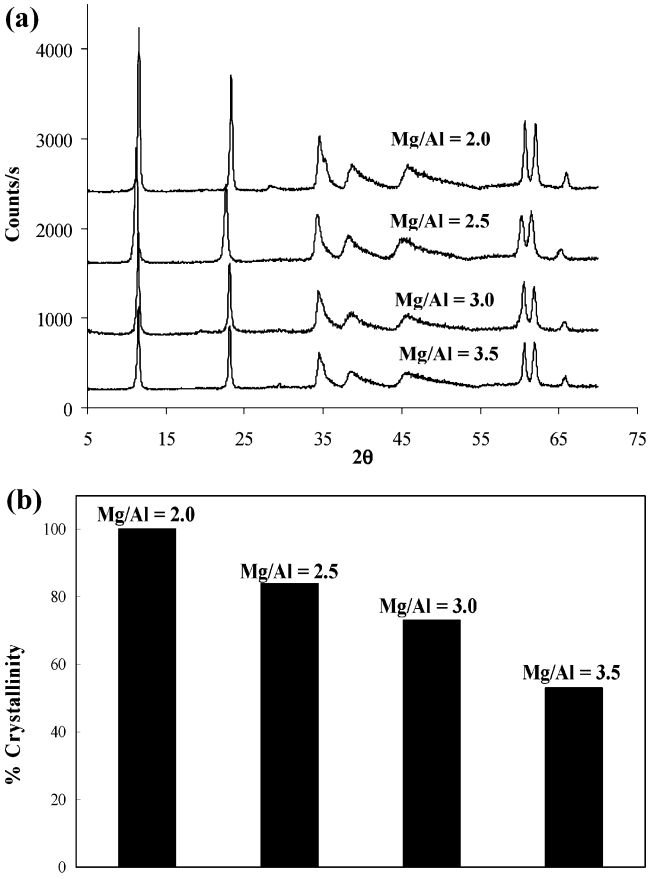

Figure 1. (a) Powder X-ray diffraction patterns of hydrotalcite of varying Mg/Al molar ratios synthesized at 140 °C hydrothermal treatment temperature and 11 h aging time. (b) Effect of the Mg/Al molar ratio of hydrotalcite on crystallinity at 140 °C and 11 h aging time.

and time under autogenous water vapor pressure. After the hydrothermal treatment, the precipitate formed was filtered and washed thoroughly with hot distilled water until the pH of the filtrate was 7. The washed precipitate was dried in an oven at 80 °C for 12 h.

Powder X-ray Diffraction (P-XRD). Powder X-ray diffraction patterns of the hydrotalcites were recorded using Phillips X'Pert MPD system equipped with XRK 900 reaction chamber, using Ni-filtered Cu Kα radiation (λ = 1.54050 A°) over a 2θ range of 0−70°. The full width in half-maxima (FWHM) of the (003) (2θ = 11.2°) and (006) (2θ = 22.5°) planes were calculated to compare the crystallite size of hydrothermally treated (70−140 °C) hydrotalcite samples (Mg/Al molar ratios of 2.0−3.5) prepared at different times. The percentage crystallinity of the samples after hydrothermal treatment was compared to the commercially available hydrotalcite (Pural MG70, supplied by SASOL, Germany) at a Mg/Al molar ratio of 2.3. The higher crystallinity of the hydrothermally treated samples at 140 °C and 11 h aging time was observed in the present study as compared to the commercially available sample (Figure 1; Supporting Information). It is well-known that the crystallinity of the hydrotalcite is significantly affected by the synthesis procedure and other factors such as aging time and temperature. To minimize the error in results observed in the present study because of the synthesis procedure and other factors, the percentage crystallinity of hydrotalcite at different hydrothermal treatment temperatures and crystallization times were calculated by comparing the summation of integral intensities of the (003) and (006) planes, and the sample having maximum intensities of the (003) and (006) planes in the present study was considered as a 100% crystalline sample. A similar procedure has been followed in the literature.[27,28] The crystallite size of hydrotalcite was calculated using the FWHM values of the (003) diffraction peaks (2θ = 11.2°), according to Scherrer's formula,

$$\text{crystallite size} = K\lambda/B\cos\theta$$

where K = shape factor (0.9 for hydrotalcite), λ = the wavelength of Cu Kα radiation (0.15405 nm), θ = Bragg diffraction angle, and B is the difference in the integral profile width of the standard and experimental samples. Silicon was used as a standard sample.

Fourier Transform Infrared (FT-IR) Spectra. The FT-infrared spectra of the hydrotalcite samples were recorded using a Perkin−Elmer Spectrum GX Fourier transform infrared spectrophotometer (FT-IR) system in the region of 400−4000 cm^{-1} using KBr pellets.

Thermogravimetric Analysis (TGA). Thermogravimetric analysis (TGA) was carried out using Mettler TGA/SDTA 851e instrument in flowing nitrogen or argon (flow rate = 50 mL/min), at a heating rate of 10 °C/min, and the data were processed using Star^e software.

Scanning Electron Microscopy (SEM) Analysis. Scanning electron microscopy (SEM) images of the hydrotalcite samples were taken on a microscope (Leo Series VP1430, Germany) having silicon detector equipped with energy-dispersive X-ray (EDX) facility (Oxford instruments). The samples were coated with gold using sputter coating to avoid charging. Analysis was carried out at an accelerating voltage of 15 kV.

Surface Area Measurements. The surface area of hydrotalcite samples was determined from the N_2 adsorption data measured at 77 K using Micromeritics, ASAP 2010 USA. The samples were activated at 80 °C for 4 h under vacuum (5 mmHg) prior to N_2 adsorption measurements. The specific surface area of the samples was calculated from the N_2 adsorption isotherms according to the Brunauer, Emmett, Teller (BET) method. The pore-size distribution of hydrotalcite samples was calculated from desorption branch using the Barrett, Joyner, and Halenda method.[29]

Results and Discussion

Powder X-ray Diffraction (P-XRD). The P-XRD patterns of the hydrotalcite samples having varying Mg/Al ratios (2.0, 2.5, 3.0, and 3.5) synthesized at 140 °C hydrothermal treatment temperatures and 11 h aging time are shown in Figure 1a. The presence of CO_3^{2-} anions in the interlayer gallery of hydrotalcite is confirmed by the characteristic basal spacing d_{003} = 7.65A°. The sharp and symmetric basal reflections of the (003) and (006) planes at low 2θ values (11−23°) and broad, asymmetric reflections at higher 2θ values (34−66°) were observed in the P-XRD patterns.[1,30] Other crystalline phases were not identified in the P-XRD patterns of all hydrotalcite samples synthesized under the studied hydrothermal treatment conditions (Figure 1a). The crystallization of hydrotalcite of varying Mg/Al molar ratios was significantly affected by hydrothermal treatment temperature and time. Poor crystallinity of hydrotalcite samples was observed prior to subjecting the precipitate for hydrothermal treatment. However, the crystallinity of samples increased significantly after hydrothermal treatment. These observations were supported by percentage crystallinity data for each sample (Figure 2).

The effect of hydrothermal treatment temperature (70, 110, and 140 °C) and time (0−11 h) on the crystallinity of hydrotalcite samples of different Mg/Al molar ratio is shown in Figure 2. The crystallinity of hydrotalcite was observed to

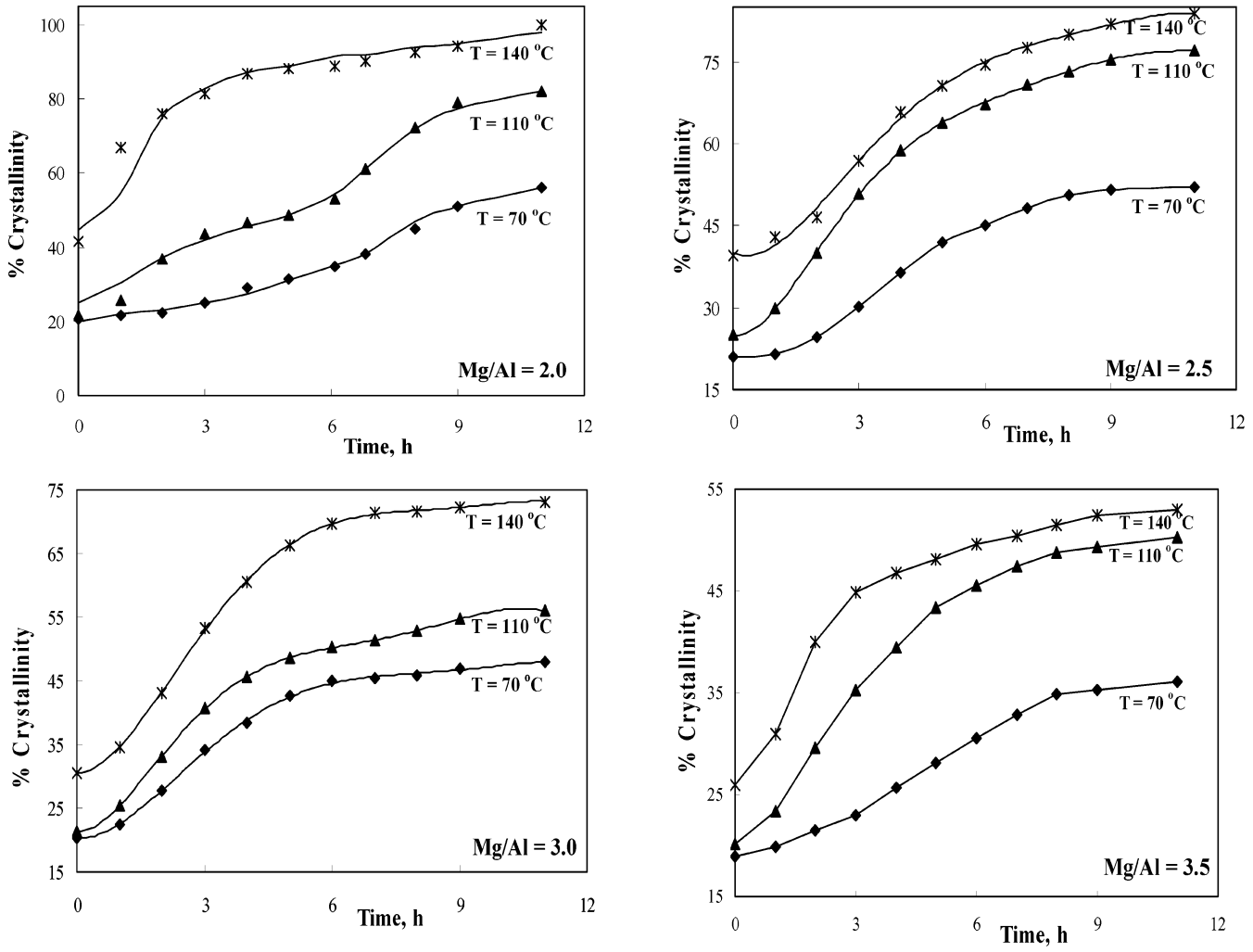

Figure 2. Effect of hydrothermal treatment temperatures and aging time on the crystallinity of hydrotalcite with Mg/Al molar ratios of 2.0−3.5.

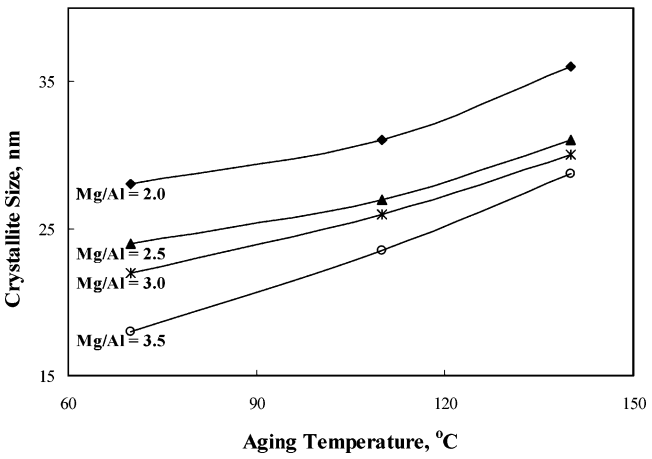

Figure 3. Effect of the Mg/Al molar ratio of hydrotalcite on crystallite size at different hydrothermal treatment temperatures and 11 h aging time.

increase slowly up to 1 h aging time followed by a sharp increase in the time range of 2−6 h. After 6 h, the time dependence of crystallinity was less evident, whereas temperature seemed to be a crucial parameter affecting the hydrothermal crystallization. For example, initially, crystallinity of the hydrotalcite was calculated to be 20%, and then it increased up to 56% at 70 °C, 82% at 110 °C, and 100% at 140 °C after 11 h crystallization time for the hydrotalcite at a Mg/Al molar ratio of 2.0 (Figure 2). The crystallinity of hydrotalcite at a Mg/Al ratio of 3.5 was observed to be 36% at 70 °C, and then it increased up to 53% at 140 °C and 11 h crystallization time. A similar effect of temperature on crystallinity of hydrotalcite samples having Mg/Al molar ratios of 2.5 and 3.0 were observed. The maximum crystallinity was observed at 140 °C for all samples. The aging time of the hydrotalcite decreased significantly with the increase in temperature. The maximum crystallinity of hydrotalcite (Mg/Al molar ratio of 2.0) was calculated as 56% at 70 °C and 11 h aging time; however, similar crystallinity was achieved by increasing the hydrothermal treatment temperature to 140 °C within 1 h aging time. The increase in crystallinity of hydrotalcite with temperature could be explained in terms of the rate of crystal growth that is directly proportional to the hydrothermal treatment temperature under identical reaction conditions. Therefore, it is expected that higher temperature will result in crystalline material with larger particles size.

The crystallization curves shown in Figure 2 exhibit the typical characteristic of a crystallization curve with the first stage corresponding to a nucleation or induction period followed by crystal growth in the second stage. Initially, formation of nuclei takes place on the addition of metal salts solution into the anionic solution at constant pH, which is simultaneously followed by the crystal growth during the addition process. The conventional nucleation period could be divided into two separate regions: one is the induction period, in which no crystal growth occurs,

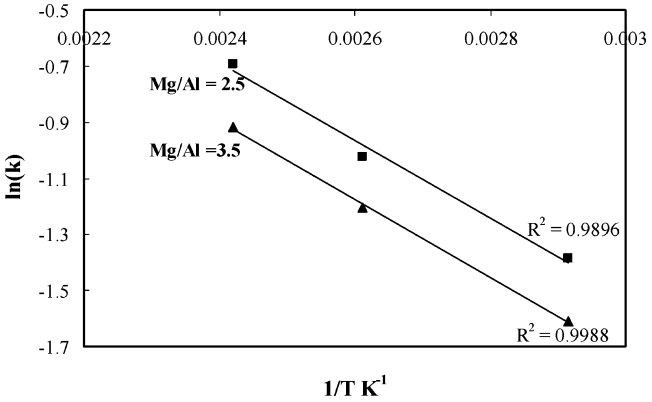

Figure 4. Arrhenius plot.

and the other is transition period, in which slow crystal growth is observed. The formation of the nuclei during the induction period is an energetically activated process,[31] and generally, a small number of nuclei are responsible for the large crystallite size of the hydrotalcite. A shorter nucleation period favors narrow crystal-size distribution.[28,32] The higher rate of nucleation as compared to the rate of crystal growth could be responsible for poor crystallinity observed at lower hydrothermal treatment temperature and 0 h aging time.[1] Therefore, a high hydrothermal treatment temperature and slow addition process favors the adsorption of added metal ions on the preformed crystal particles rather than the formation of the new nuclei.[15]

The effect of the Mg/Al molar ratio on the crystallinity of hydrotalcite samples was studied at 140 °C hydrothermal treatment temperature and 11 h aging time (Figure 1b). The peaks in P-XRD patterns of hydrotalcite became sharper and more intense on decreasing the Mg/Al molar ratio of hydrotalcite. This shows that the crystallinity of hydrotalcite samples decreased with an increase in the Mg/Al molar ratio under hydrothermal treatment conditions. The crystallinity of hydrotalcites samples was calculated as 100% for a Mg/Al molar ratio of 2.0, 84% for a Mg/Al molar ratio of 2.5, 73% for a Mg/Al molar ratio of 3.0, and 53% for a Mg/Al molar ratio of 3.5 at 140 °C and 11 h crystallization time. The decrease in the crystallinity on increasing the Mg/Al molar ratio of hydrotalcite samples is due to the increase in the amount of divalent cations (Mg^{2+}), which have ionic radii of 0.65 A° that favor the formation of brucite by replacing the smaller ionic radii trivalent cations (Al^{3+}).[33] The increase in Mg/Al molar ratio of hydrotalcite also results in a decrease in charge density on layers due to the decrease in Coulombic attractive force between the negatively charged interlayer anions and positively charged brucite-like layers.[1]

The effect of hydrothermal treatment temperatures on crystallite size of hydrotalcite samples of different Mg/Al molar ratios at 11 h is shown in Figure 3. The crystallite size of hydrotalcite samples increased on the increase in hydrothermal treatment temperature and crystallization time. For a Mg/Al molar ratio of 2.0 and 70 °C, the crystallite size of the hydrotalcite was observed to be 28 nm, which increased to 30 nm at 110 °C, and 36 nm (±1 nm) at 140 °C after 11 h. The crystallite size of hydrotalcite samples was observed to decrease on increasing the Mg/Al molar ratio. At a Mg/Al molar ratio of 3.5 and 70 °C, the crystallite size of hydrotalcite was observed to be 18 nm and increased up to 24 nm at 110 °C and 29 nm at 140 °C. These results show that the hydrothermal treatment of hydrotalcite samples at higher temperature gives a larger crystal size in a shorter crystallization time. The effect of temperature on the rate of crystal growth could be expressed[28,34] by eq 1

$$\frac{dL}{dt} = C[1 - \exp(-RT)] \quad (1)$$

where C = constant, L = crystal size, and T = hydrothermal treatment temperature.

According to eq 1, higher temperature results in larger crystal size and the rate of crystal growth is proportional to the hydrothermal treatment temperature under identical synthesis conditions. The crystallite size of the hydrotalcite is also affected by the total number of nuclei produced during the crystallization process and the length of the nucleation period. The crystallite-size distribution in a wide range is also observed at different hydrothermal treatment temperatures and increasing aging time. The effect of the Mg/Al ratio on the crystallite size of hydrotalcite could be explained in terms of the presence of cations. The presence of a larger number of trivalent cations (Al^{3+}) in the layers enhances the rate of stacking of the layers.

Kinetics of Crystallization. The Avrami−Erofeev model[35,36] provides a correlation between crystalline volume fraction (α) and crystallization time (t) (eq 2) and was applied for fitting the observed crystallization data. The Avrami−Erofeev model (nucleation-growth model) assumes that the progress of the crystallization process follows the nucleation and growth mechanism by considering the coalescence and ingestion of other nuclei as the new phase grows. If the samples are divided into small equal volumes, then random nucleation is assumed with uniform nucleus formation in equal volumes with respect to time. This model also assumed a limited number of potential sites for nucleation. The kinetic data of the crystallization process for the synthesis of hydrotalcite at Mg/Al molar ratios from 2.0 to 3.5 at 70−140 °C temperature were fitted into eq 2.

$$\alpha = 1 - \exp[-(kt)^n] \quad (2)$$

where α = degree of crystallinity, k = rate constant, t = aging time, and n = Avrami exponent.

To solve eq 2, one must take logarithms twice as follows:

$$\ln[-\ln(1 - \alpha)] = n \ln t + n \ln k \quad (3)$$

The values of k and n were calculated from a plot of ln[−ln(1 − α)] vs ln t (Sharp−Hancock plot), which gives a straight line of slope n and intercept n ln k. The calculated Avrami−Erofeev parameters (k and n) at 70, 110, and 140 °C treatment temperatures are given in Table 1. The value of k was observed to increase with an increase in the temperature. At 70 °C and a

Table 1. Avrami−Erofeev Equation Parameters for Kinetics of Crystallization of Hydrotalcite at Different Temperatures

	T = 70 °C			T = 110 °C			T = 140 °C			
Mg/Al molar ratio	k, h^{-1}	n	R^2	k, h^{-1}	n	R^2	k, h^{-1}	n	R^2	activation energy, kJ/ mol
2.0	0.18	0.5	0.90	0.26	0.7	0.92	0.55	0.5	0.99	16.1
2.5	0.25	0.7	0.99	0.36	0.6	0.99	0.50	0.6	0.98	11.5
3.0	0.26	0.5	0.98	0.31	0.5	0.98	0.42	0.6	0.98	10.5
3.5	0.20	0.5	0.97	0.27	0.5	0.98	0.40	0.5	0.97	11.6

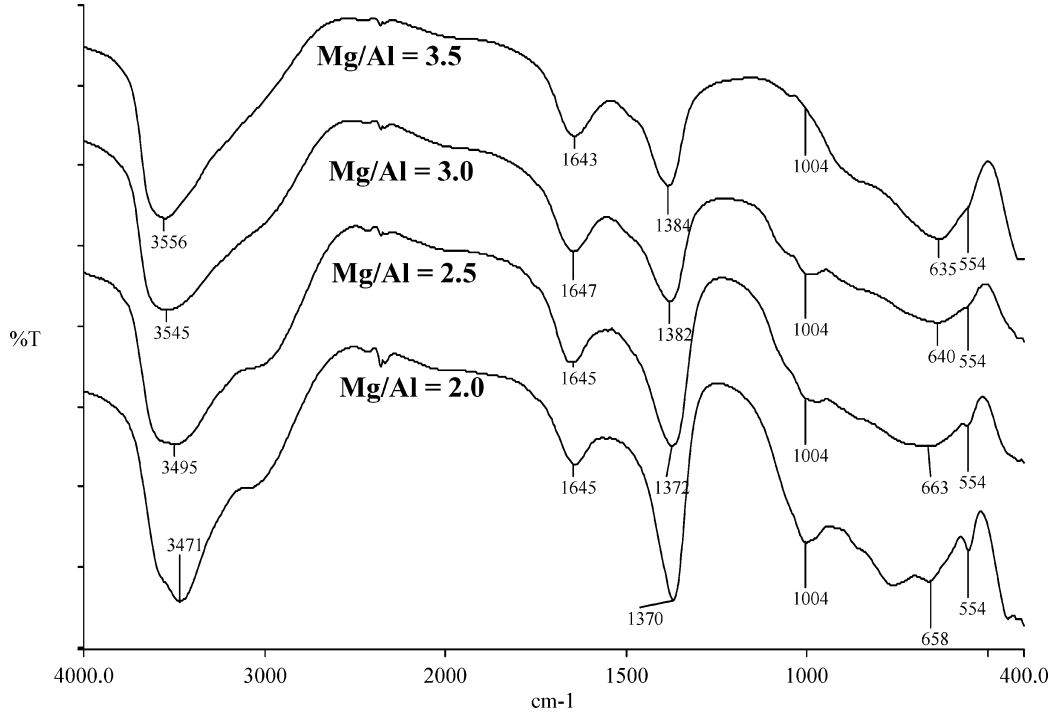

Figure 5. FT-IR spectra of hydrotalcite with Mg/Al molar ratios of 2.0−3.5 at 140 °C and 11 h aging time.

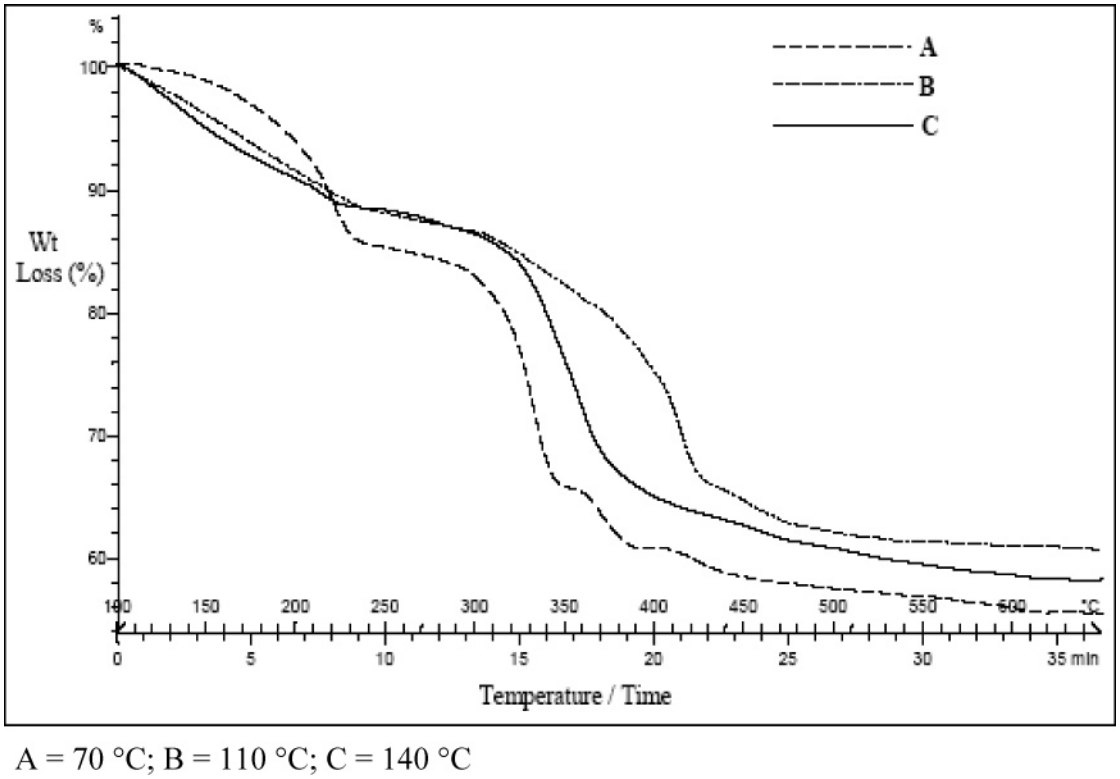

A = 70 °C; B = 110 °C; C = 140 °C

Figure 6. Thermogravimetric analysis (TGA) of hydrotalcite at a Mg/Al molar ratio of 2.0 at different temperatures and 11 h aging time.

Mg/Al molar ratio of hydrotalcite of 2.0, k was found to be 0.18 h^{-1}, which increased to 0.26 h^{-1} at 110 °C and to 0.55 h^{-1} at 140 °C. However, no significant change was observed in the value of n, which was found to be in the range of 0.5−0.7. The increase in k values on increasing hydrothermal treatment temperature indicates the faster crystallization process at higher temperature in a short crystallization time. The rate constant (k) is a strong function of temperature; as temperature increases, the rate of the formation of nucleation sites also increases, which results in faster crystallization in a short time. The Avrami exponent contains information regarding the mechanism of the crystallization process. The observed value of n in the range of 0.5−0.7 is a clear indication of random nuclei formation and two-dimensional nuclei growth.[37] The value of n in the range of 0.5−0.7 suggests that the overall rate of crystallization does not depend on the rate of formation of nucleation sites for crystal growth on the surface of crystallite. However, the overall rate of crystallization depends on the rate

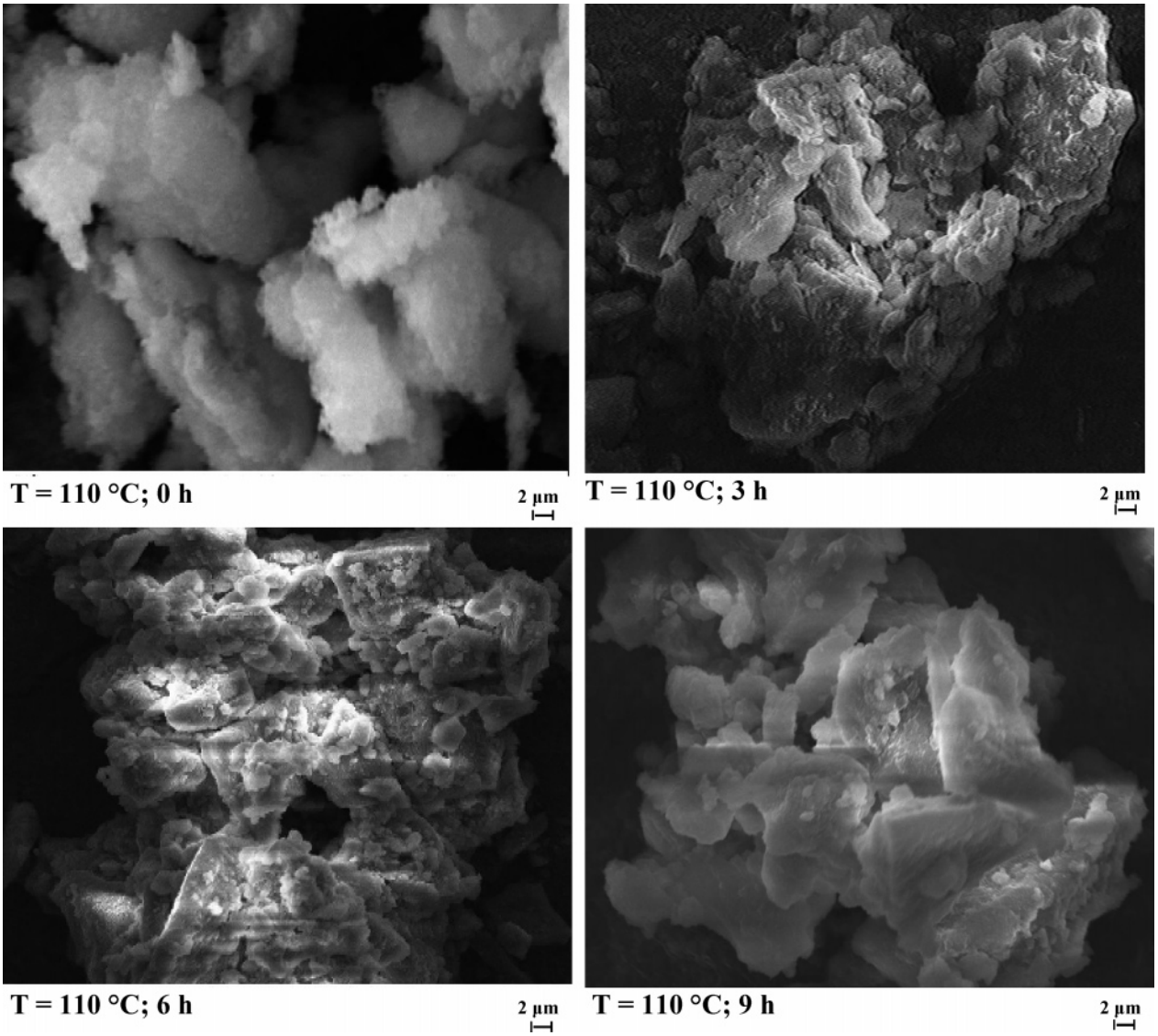

Figure 7. Scanning electron microscopy (SEM) images of hydrotalcite at a Mg/Al molar ratio of 2.0 at different aging times and 110 °C.

of diffusion of reactive species through the solution to crystallite site or dissolution of starting materials.[38] The activation energy for the crystallization process was calculated from the slope of plots of ln k vs $1/T$ (Arrhenius plot, Figure 4). The activation energy was found to be 16.1, 11.5, 10.5, and 11.6 kJ/mol for the hydrotalcite samples with Mg/Al molar ratios of 2.0, 2.5, 3.0, and 3.5, respectively. The difference between the values of activation energy at varying Mg/Al molar ratios suggests that only homogeneous nucleation takes place at early stages of transition state and that the number of nuclei remains constant thereafter. The energy required for the formation of the nuclei during the induction period can be calculated from the difference between the values of activation energy.

FT-infrared (FT-IR) Spectra. The FT-IR spectra of the hydrotalcite samples with Mg/Al molar ratios of 2.0−3.5 at 140 °C and 11 h are shown in Figure 5. The FT-IR spectra obtained for all samples are in good agreement, with only slight variations in the peak positions as compared to the data available in the literature.[1] The broad peak at around 3500 cm^{-1} is attributed to the H-bonding stretching and bending vibrations of the OH group in the brucite-like layer. The increase in the Mg/Al molar ratio of hydrotalcite resulted in slight shifting of the OH-stretching bands (3500 cm^{-1}) toward higher frequencies due to the major role of the Mg−OH stretching mode.[1,33] The shoulder present around 3000 cm^{-1} is attributed to hydrogen bonding between H_2O and interlayer CO_3^{2-} anions. The intensity of this shoulder increases with the crystallinity of hydrotalcite, indicating stronger layer−interlayer interactions and a well-ordered interlayer region.[25] The hydrogen stretching and bending frequencies were found to increase with an increase in the Mg/Al ratio of hydrotalcite from 2.0 to 3.5. The appearance of a shoulder at 1640 cm^{-1} is characteristic bands of H_2O. The sharp, intense vibrational band of carbonates (antisymmetric stretching, ν_3) that appears at 1370 cm^{-1} could be assigned to interlayer carbonates (chelating or bridging bidentate). However, for the samples with a lower degree of crystallinity, an asymmetric or split ν_3 vibrational band of carbonates was observed. The intensity of the band at 1370 cm^{-1} also decreased in the poor crystalline samples. The bands at 950 cm^{-1} for the deformation of Al−OH and at 760 cm^{-1} for the Al−OH translation were also observed. The peak at about 650 cm^{-1} (ν_4) is assigned to the in-plane carbonate bending. On increase in the Mg/Al molar ratio of hydrotalcite, the broadening of the peak at about 650 cm^{-1} was observed. The band at 554 cm^{-1} is assigned to the translation modes of hydroxyl groups, influenced by Al^{3+} cations (Mg/Al−OH translation).[39]

Thermogravimetric Analysis (TGA). Thermogravimetric (TG) curves of hydrotalcite samples with a Mg/Al molar ratio

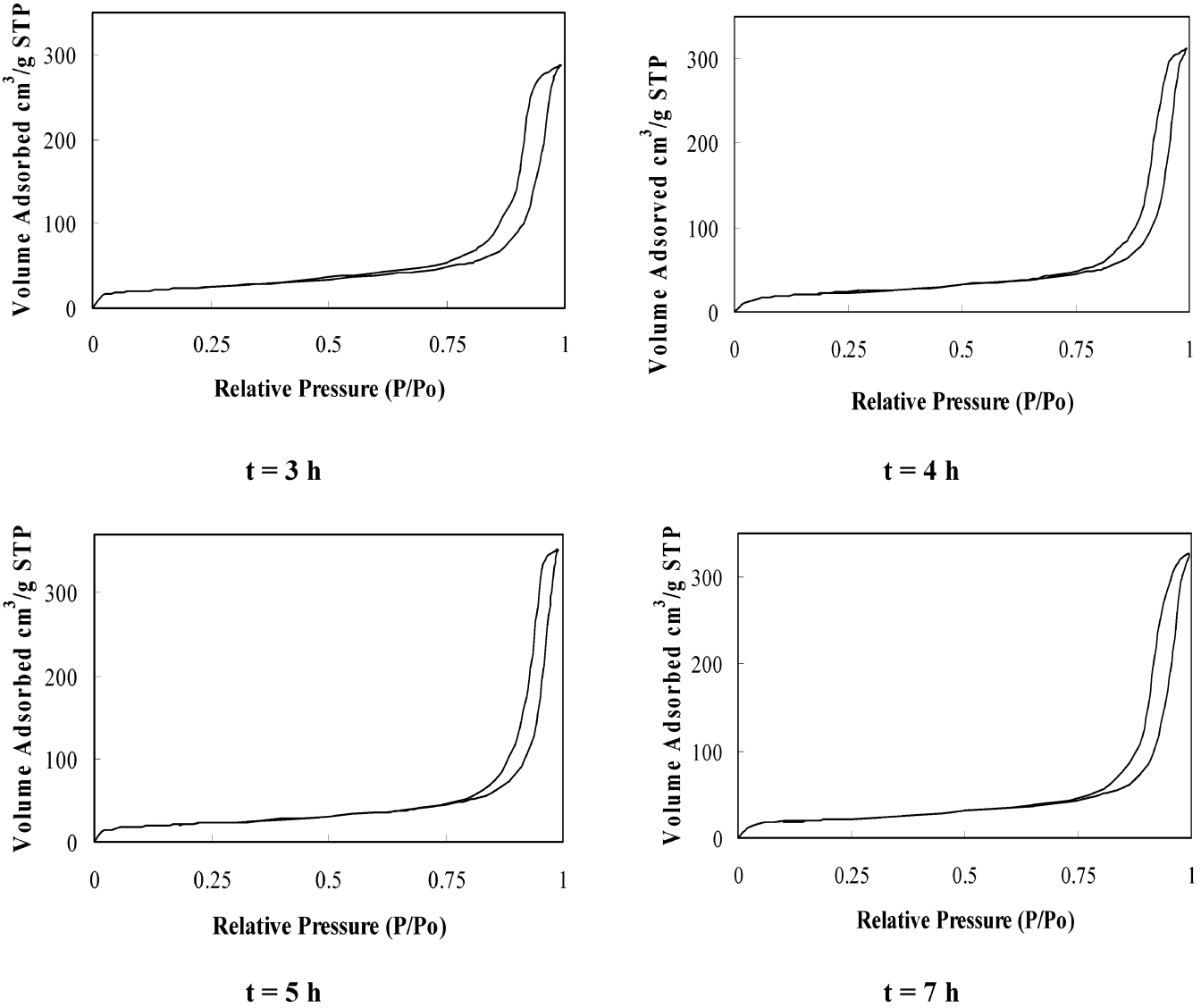

Figure 8. N_2 adsorption−desorption isotherms at 77 K for hydrotalcite at a Mg/Al = 3.5 at 70 °C and different aging times.

Table 2. BET Surface Area (S_{BET}) and Pore-Size Distribution for Hydrotalcite at a Mg/Al Molar Ratio of 3.5 at 70 °C

aging time, h	surface area (S_{BET}), $m^2\ g^{-1}$	pore volume (V_p), $cm^3\ g^{-1}$	pore diameter, nm
3	85	0.41	9.3
4	78	0.44	9.8
5	76	0.43	9.6
7	75	0.44	11.5

2.0 at 70, 110, and 140 °C hydrothermal treatment temperatures are shown in Figure 6. Three-stage weight losses were observed in the TG pattern of hydrotalcite treated at 70 °C. The weight loss (15% of initial amount) in the first stage observed at around 220 °C was attributed to the removal of loosely bound water molecules from the hydrotalcite pores. The second weight loss (38%) was observed in the temperature range of 330−380 °C by the removal of OH^- groups from the interlayer, which is bonded mostly with Mg^{2+} [Mg−(OH)−Mg] and [Al−(OH)−Mg]. In the third-stage weight loss (44%), decarbonation of carbonate anion present in the interlayer space was observed in the temperature range of 400−550 °C. After removal of CO_3^{2-} anions from the interlayer space, the material becomes amorphous metastable mixed solid oxides.[40] The weight loss in two steps was observed in TG curves of the samples treated at 110 and 140 °C temperatures. The samples treated at higher temperature show a lower weight loss in TGA as compared to the samples treated at 70 °C, indicating higher stability of the hydrotalcite at higher hydrothermal treatment temperature, which is related to the enhanced crystallinity and stacking of the layers.

Scanning Electron Microscopy (SEM) Analysis. The SEM images of hydrotalcite samples at a Mg/Al molar ratio of 2.0 were recorded to observe the effect of aging time on the morphology of the material. The micrographs at different aging times are shown in Figure 7. From the micrographs of hydrotalcite, a well-developed layered and platelet structure of the hydrotalcite was observed. However, a spongy type structure is exhibited due to overlapping of such platelets. The SEM images of the hydrotalcite showed a gradual crystallization during the hydrothermal treatment conditions. The crystallinity of the hydrotalcite was observed to be very poor at 0 h aging time and 110 °C hydrothermal treatment temperature; however, as aging time increases from 0 to 10 h, the crystallinity of the hydrotalcite also increased. The observations from the SEM images were in good agreement with P-XRD patterns and surface area measurements. These results confirmed an increase

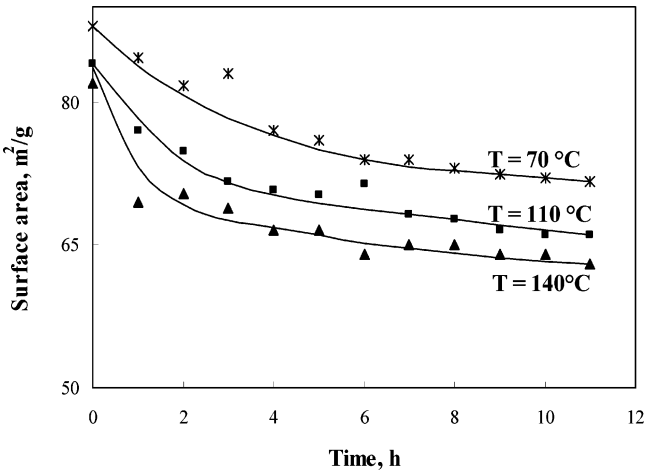

Figure 9. Effect of hydrothermal treatment temperature and time on the surface area of hydrotalcite at a Mg/Al molar ratio of 3.5.

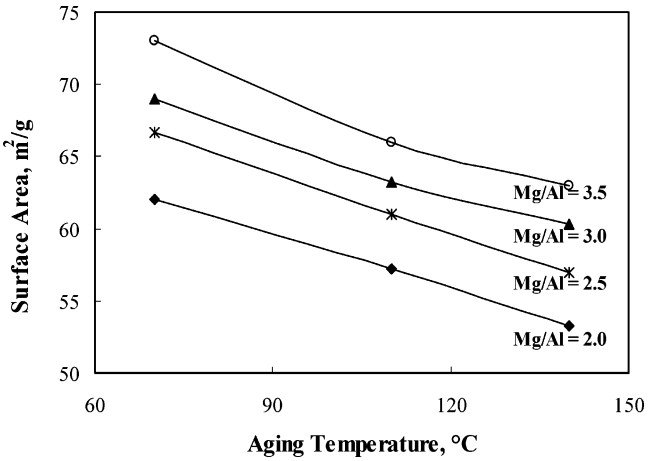

Figure 10. Effect of the Mg/Al molar ratio of hydrotalcite on the surface area at different hydrothermal treatment temperatures and 11 h.

in the crystallinity of the hydrotalcite samples at Mg/Al ratios of 2.0−3.5 under hydrothermal treatment conditions.

Surface Area Measurements. Nitrogen adsorption−desorption isotherms of the hydrotalcite at a Mg/Al molar ratio of 3.5 with respect to time measured at liquid nitrogen temperature (77 K) are shown in Figure 8. The shapes of all of the isotherms are type IV according to the IUPAC classification and represent a mesoporous adsorbent with strong adsorbent−adsorbate interaction.[41] Figure 8 shows that the desorption started immediately after completion of adsorption (H1 hysteresis). The hysteresis is associated with capillary condensation in the mesostructures. The slight changes in the hysteresis loops were observed due to the synthesis methodology and hydrothermal treatment conditions related to the shape and homogeneity of the pore size. At 3 h aging time, the loop closes at around 0.5 relative pressure (P/P_o) with a small plateau at high P/P_o, which attributes to the mesoporous nature of these samples. As the aging time increases, the relative pressure for the loop closing also increases toward the higher value (Figure 8). The hysteresis loops are almost vertical and parallel over an appreciable range of relative pressure and such shape of the loops suggests aggregates of platelike particles leading to slit-shaped pores of the hydrotalcite.[42]

Average pore-size distribution and surface areas for the hydrotalcite samples having a Mg/Al molar ratio of 3.5 synthesized at 70 °C with 3−7 h aging time are given in Table 2. The pore diameter was observed to increase on increasing time. For example, pore diameter was observed to increase from 9.3 to 11.5 nm on increasing the aging time from 3 to 7 h. The increase in pore diameter could be attributed to the difference in the nature of aggregation of primary particles (constituent crystallites) during the crystallization process. As the crystallization time increased, the primary particles of hydrotalcite grew, resulting in larger pore diameters. However, significant changes were not observed in the pore volume of hydrotalcite samples at a Mg/Al molar ratio of 3.5 with respect to time at 70 °C.

Surface area (S_{BET}) of the hydrotalcite samples was observed to decrease with an increase in aging time and hydrothermal treatment temperature (Figure 9). The surface area of the hydrotalcite without any hydrothermal treatment was found to be 87 m^2g^{-1}. However, the surface area decreased from 87 to 73, 66, and 63 m^2g^{-1} at 70, 110, and 140 °C hydrothermal treatment temperatures, respectively. Initially, up to 3 h aging time at all hydrothermal treatment temperatures, the surface area of the samples decreased sharply. A slow decrease in the surface area of hydrotalcite was observed during 3−9 h, and after 9 h, no significant effect of time was observed on the surface area of hydrotalcite.

The effect of the Mg/Al molar ratio of hydrotalcite on the surface area at different hydrothermal treatment temperatures and 11 h aging time is shown in Figure 10. The surface area of hydrotalcite increased from 62 to 73 m^2g^{-1} on the increase in the Mg/Al molar ratio from 2.0 to 3.5 at 70 °C and 11 h aging time. Similar trends in the variation of the surface area of hydrotalcite samples were observed at 110 and 140 °C. The increase in the surface area on increasing Mg/Al molar ratio is attributed to the observed decrease in the calculated crystallinity and crystallite sizes of hydrotalcite from P-XRD patterns. Generally, smaller crystallite sizes of hydrotalcites yield larger surface areas.

The hydrothermal treatment conditions have influenced the surface area of hydrotalcite significantly, since these textural properties are directly related to the agglomeration of the particles and particle size.[43] The decrease in the surface area of the hydrotalcite on increasing the aging time and temperature could be corelated to the simultaneous nucleation, which enhanced the crystallinity of material and larger crystallite size, which is in good agreement with the observed P-XRD data. The other reason for the lower surface area is face-to-face or card-house type aggregation of crystallites, which is responsible for the lower specific surface area of hydrotalcite at higher hydrothermal treatment temperature and crystallization time.[16,44] It is assumed that the rapid enhancement in the crystallinity leads to lower probability for face-to-face aggregates formation, which results in the increasing specific surface area of hydrotalcite during short aging time and low hydrothermal treatment temperature.[18]

Conclusions

The crystallization of hydrotalcite (Mg/Al molar ratio = 2.0−3.5) was significantly affected by the hydrothermal treatment temperature (70−140 °C) and time (0−11 h). The crystallite size of hydrotalcite samples was observed to decrease on increasing the Mg/Al molar ratio. At a Mg/Al molar ratio of 3.5 and 70 °C, the crystallite size of hydrotalcite was observed to be 18 nm, which increased up to 24 nm at 110 °C and 29 nm at 140 °C. From the kinetic data, the activation energy for the crystallization of hydrotalcite was found to be 16.1, 11.5,

10.5, and 11.6 kJ/mol for the hydrotalcite samples with Mg/Al molar ratios of 2.0, 2.5, 3.0, and 3.5, respectively. The surface area (S_{BET}) of the hydrotalcite samples was observed to decrease with an increase in aging time and hydrothermal treatment temperature. Surface area values decreased from 87 to 73, 66, and 63 m^2g^{-1} at 70, 110, and 140 °C, respectively. The surface area of hydrotalcite increased from 62 to 73 m^2g^{-1} on the increase in the Mg/Al molar ratio from 2.0 to 3.5 at 70 °C and 11 h aging time. The pore diameters were observed to increase on increasing the aging time.

Acknowledgment

The authors thank Dr. P. K. Ghosh, Director, CSMCRI, Bhavnagar, India, for encouraging this publication; Dr. P. Bhatt for P-XRD analysis; V. Agrawal for FT-IR analysis; Harishchandra D. J. for TGA; Mr. Ranjith S. and Prashant K.P. for surface area measurements; and Network Project on Catalysis, Council of Scientific and Industrial Research (CSIR), New Delhi, India, for financial support. S.K.S. thanks CSIR, New Delhi, for the award of a Senior Research Fellowship.

Supporting Information Available: Included in the Supporting Information is P-XRD patters of hydrotalcite samples at varying Mg/Al ratios. This material is available free of charge via the Internet at http://pubs.acs.org.

Literature Cited

(1) Cavani, F.; Trifiro, F.; Vaccari, A. Hydrotalcite-type anionic clays: Preparation, properties and applications. *Catal. Today* **1991**, *11*, 173−301.

(2) Ulibarri, M. A.; Pavlovic, I.; Barriga, C.; Hermosin, M. C.; Cornejo, J. Adsorption of anionic species on hydrotalcite-like compounds: Effect of interlayer anion and crystallinity. *Appl. Clay Sci.* **2001**, *18*, 17−27.

(3) Winter, F.; van Dillen, A. J.; de Jong, K. P. Supported hydrotalcites as highly active solid base catalysts. *Chem. Commun.* **2005**, 3977−3979.

(4) Roelofs, J. C. A. A.; Lensveld, D. J.; van Dillen, A. J.; de Jong, K. P. On the structure of activated hydrotalcites as solid base catalysts for liquid-phase aldol condensation. *J. Catal.* **2001**, *203*, 184−191.

(5) Climent, M. J.; Corma, A.; Iborra, S.; Epping, K.; Velty, A. Increasing the basicity and catalytic activity of hydrotalcites by different synthesis procedures. *J. Catal.* **2004**, *225*, 316−326.

(6) Nikolopoulos, A. A.; Jang, B. W. L.; Spivey, J. J. Acetone condensation and selective hydrogenation to MIBK on Pd and Pt hydrotalcite-derived Mg−Al mixed oxide catalysts. *Appl. Catal., A* **2005**, *296*, 128−136.

(7) Ramani, A.; Chanda, B. M.; Velu, S.; Sivasanker, S. One-pot synthesis of coumarins−Catalysis by the solid base, calcined Mg−Al hydrotalcite. *Green Chem.* **1999**, 163−165.

(8) Khan, F. A.; Dash, J.; Satapathy, R.; Upadhyay, S. K. Hydrotalcite catalysis in ionic liquid medium: A recyclable reaction system for heterogeneous Knoevenagel and nitroaldol condensation. *Tetrahedron Lett.* **2004**, *45*, 3055−3058.

(9) Tamura, H.; Chiba, J.; Ito, M.; Takeda, T.; Kikkawa, S. Synthesis and characterization of hydrotalcite−ATP intercalates. *Solid State Ionics* **2004**, *172*, 607−609.

(10) Schmidt, F. New catalyst preparation technologies−Observed from an industrial viewpoint. *Appl. Catal., A* **2001**, *221*, 15−21.

(11) Jobbagy, M.; Regazzoni, A. E. Anion-exchange equilibrium and phase segregation in hydrotalcite systems: Intercalation of hexacyanoferrate-(III) ions. *J. Phys. Chem. B* **2005**, *109*, 389−393.

(12) Vaccari, A. Clays and catalysis: A promising future. *Appl. Clay Sci.* **1999**, *14*, 161−198.

(13) Srivastava, V. K.; Bajaj, H. C.; Jasra, R. V. Solid base catalysts for isomerization of 1-methoxy-4-(2-propen-1-yl)benzene to 1-methoxy-4-(1-propen-1-yl)benzene. *Catal. Commun.* **2003**, *4*, 543−548.

(14) Figueras, F.; Lopez, J.; Sanchez-Valente, J.; Vu, T. T. H.; Clacens, J. M.; Palomeque, J. Isophorone isomerization as model reaction for the characterization of solid bases: Application to the determination of the number of sites. *J. Catal.* **2002**, *211*, 144−149.

(15) Evans, D. G.; Duan, X. Preparation of layered double hydroxides and their applications as additives in polymers, as precursors to magnetic materials and in biology and medicine. *Chem. Commun.* **2006**, 485−496.

(16) Yun, S. K.; Pinnavaia, T. J. Water content and particle texture of synthetic hydrotalcite-like layered double hydroxides. *Chem. Mater.* **1995**, *7*, 348−354.

(17) Allada, R. K.; Pless, J. D.; Nenoff, T. M.; Navorotsky, A. Thermochemistry of hydrotalcite-like phases intercalated with CO_3^{2-}, NO_3^-, Cl^-, I^-, and ReO_4^-. *Chem. Mater.* **2005**, *17*, 2455−2459.

(18) Bravo-Suarez, J. J.; Paez-Mozo, E. A.; Oyama, S. T. Microtextural properties of layered double hydroxides: a theoretical and structural model. *Microporous Mesoporous Mater.* **2004**, *67*, 1−17.

(19) Othman, M. R.; Rasid, N. M.; Fernando, W. J. N. Effects of thermal treatment on the micro-structures of co-precipitated and sol−gel synthesized (Mg−Al) hydrotalcites. *Microporous Mesoporous Mater.* **2006**, *93*, 23−28.

(20) Kloprogge, J. T.; Hickey, L.; Frost, R. L. The effects of synthesis pH and hydrothermal treatment on the formation of zinc aluminum hydrotalcites. *J. Solid State Chem.* **2004**, *177*, 4047−4057.

(21) Darder, M.; Blanco, M. L.; Aranda, P.; Leroux, F.; Hitzky, E. R. Bio-nanocomposites based on layered double hydroxides. *Chem. Mater.* **2005**, *17*, 1969−1977.

(22) Xu, Z. P.; Lu, G. Q. Hydrothermal synthesis of layered double hydroxides (LDHs) from mixed MgO and Al_2O_3: LDH formation mechanism. *Chem. Mater.* **2005**, *17*, 1055−1082.

(23) Miyata, S. Physico-chemical properties of synthetic hydrotalcites in relation to composition. *Clays Clay Miner.* **1980**, *28*, 50−56.

(24) Hickey, L.; Kloprogge, J. T.; Frost, R. L. The effects of various hydrothermal treatments on magnesium−aluminium hydrotalcites. *J. Mater. Sci.* **2000**, *35*, 4347−4355.

(25) Labajos, F. M.; Rives, V.; Ulibarri, M. A. Effect of hydrothermal and thermal treatments on the physicochemical properties of Mg−Al hydrotalcite-like materials. *J. Mater. Sci.* **1992**, *27*, 1546−1552.

(26) Kovanda, F.; Kolousek, D.; Cilova, Z.; Hulinsky, V. Crystallization of synthetic hydrotalcite under hydrothermal conditions. *Appl. Clay Sci.* **2005**, *28*, 101−109.

(27) Costantino, U.; Marmottini, F.; Nocchetti, M.; Vivani, R. New synthetic routes to hydrotalcite-like compounds−Characterization and properties of the obtained materials. *Eur. J. Inorg. Chem.* **1998**, 1439−1446.

(28) Oh, J. M.; Hwang, S. H.; Choy, J. H. The effect of synthetic conditions on tailoring the size of hydrotalcite particles. *Solid State Ionics* **2002**, *151*, 285−291.

(29) Barrett, E. P.; Joyner, L. G.; Halenda, P. P. The determination of pore volume and area distributions in porous substances. I. Computations from nitrogen isotherms. *J. Am. Chem. Soc.* **1951**, *73*, 373−380.

(30) Miyata, S. The synthesis of hydrotalcite-like compounds and their structures and physico-chemical properties. I. *Clays Clay Miner.* **1975**, *23*, 369−375.

(31) Kim, W. J.; Kim, S. D.; Jung, H. S.; Hayhurst, D. T. Compositional and kinetic studies on the crystallization of ETS-10 in the presence of various organics. *Microporous Mesoporous Mater.* **2002**, *56*, 89−100.

(32) Myatt, G. J.; Budd, P. M.; Price, C.; Hollway, F.; Carr, S. W. The influence of surfactants and water-soluble polymers on the crystallization of zeolite NaA. *Zeolites* **1994**, *14*, 190−197.

(33) Kustrowski, P.; Sulkowska, D.; Chmielarz, L.; Rafalska-Lasocha, A.; Dudek, B.; Dziembaj, R. Influence of thermal treatment conditions on the activity of hydrotalcite-derived Mg−Al oxides in the aldol condensation of acetone. *Microporous Mesoporous Mater.* **2005**, *78*, 1−22.

(34) Nayvlt, J.; Sohnel, O.; Matuchova, M.; Broul, M. *The Kinetics of Industrial Crystallization*; Chemical Engineering Monographs, Vol. 19; Elsevier: Amsterdam, The Netherlands, 1985.

(35) Avrami, M. Kinetics of phase change. 1. General theory. *J. Chem. Phys.* **1939**, *7*, 1103−1112.

(36) Avrami, M. Kinetics of phase change. 1. Transformation−time relations for random distribution of nuclei. *J. Chem. Phys.* **1940**, *8*, 212−224.

(37) Yoshinari, T.; Forbes, R. T.; York, P.; Kawashima, Y. Crystallisation of amorphous mannitol is retarded using boric acid. *Int. J. Pharm.* **2003**, *258*, 109−120.

(38) Millange, F.; Walton, R. I.; Hare, D. O. Time-resolved in situ X-ray diffraction study of the liquid-phase reconstruction of Mg−Al−carbonate hydrotalcite-like compounds. *J. Mater. Chem.* **2000**, *10*, 1713−1720.

(39) Abello, S.; Medina, F.; Tichit, D.; Ramirez, J. P.; Groen, J. C.; Sueiras, J. E.; Salagre, P.; Cesteros, Y. Aldol Condensations Over Reconstructed Mg−Al Hydrotalcites: Structure−Activity Relationships Related to the Rehydration Method. *Chem.—Eur. J.* **2005**, *11*, 728−739.

(40) Yang, W.; Kim, Y.; Liu, P. K. T.; Sahimi, M.; Tsotsis, T. T. A study by in situ techniques of the thermal evolution of the structure of a Mg−Al−CO_3 layered double hydroxide. *Chem. Eng. Sci.* **2002**, *57*, 2945−2953.

(41) Sing, K. S. W.; Everett, D. H.; Haul, R. A. W.; Moscou, L.; Pierotti, E.; Rouquerol, J.; Sieminiewska, T. Reporting physicsorption data for gas/solid systems with special reference to the determination of surface area and porosity. *Pure Appl. Chem.* **1985**, *57*, 603−619.

(42) Mohmel, S.; Kurjawski, I.; Uecker, D.; Muller, D.; Gebner, W. The influence of a hydrothermal treatment using microwave heating on the crystallinity of layered double hydroxides. *Cryst. Res. Technol*. **2002**, *37*, 359−369.

(43) Bento, P.; Labajos, F. M.; Rocha, J.; Rives, V. Influence of microwave radiation on the textural properties of layered double hydroxides. *Microporous Mesoporous Mater*. **2006**, *94*, 148−158.

(44) Albiston, L.; Franklin, K. R.; Lee, E.; Smeulders J. B. A. F. Rheology and microstructure of aqueous layered double hydroxide dispersions. *J. Mater. Chem.* **1996**, *6*, 871−877.

Received for review November 9, 2006
Revised manuscript received May 11, 2007
Accepted May 12, 2007

IE061438W